THE BALTIC JOURNAL
OF ROAD AND BRIDGE ENGINEERING

2011
6(1): 39–47

COMPARISON OF BRIDGE DYNAMIC AMPLIFICATIONS DUE TO ARTICULATED 5-AXLE TRUCKS AND LARGE CRANES

Daniel Cantero[1], Arturo González[2], Eugene J. OBrien[3]

School of Architecture, Landscape and Civil Engineering, University College Dublin, Dublin 4, Ireland
E-mails: [1]canterolauer@gmail.com; [2]arturo.gonzalez@ucd.ie; [3]eugene.obrien@ucd.ie

Abstract. Extremely heavy vehicles are becoming more common on European highways due to the increasing demand for transport of heavy goods. These vehicles require permits from the road authorities to travel over a specified route. The authorities must ensure the bridge infrastructure remains safe when traversed by these very heavy vehicles and an escort is typically used to reduce loading in long-span bridges. In the case of short- and medium-span bridges, the closely spaced axle's forces of cranes form a critical traffic load configuration that must be carefully assessed before granting a permit. In this paper, the parameters of a 3D vehicle-bridge interaction model are varied using Monte Carlo simulation to find the dynamic increment in the bridge response due to large cranes. A number of bridge spans, simply supported and fixed, and road conditions (with and without a damaged joint prior to the bridge) are tested and the bridge response is compared to conventional 5-axle trucks.

Keywords: vehicle, bridge, interaction, dynamics, articulated trucks, crane, expansion joint.

1. Introduction

Previous research has shown that site-specific traffic modelling allows more accurate bridge assessments and large reductions in characteristic loading effects calculation compared to deterministic load models found in design codes (O'Connor, Eichinger 2007). Recent improvement in Weigh-in-Motion (WIM) technology provide the road authorities with the tool necessary for assessing bridges on existing road networks (OBrien *et al.* 2008a). The frequency of extremely heavy vehicles is becoming increasingly important, with gross weights in excess of 100 tonnes being recorded daily at some sites (OBrien *et al.* 2008b). These vehicles are either large (mobile) cranes with very closely spaced axles or low loaders with much longer wheelbases. Even though they could be expected to have special permits and escort vehicles, they are found mixed with normal traffic and travelling close to the speed limit. There are a lot of theoretical investigations and experimental records on bridge dynamics due to traffic, but they are mainly focused on normal vehicle types such as 2- or 5-axle trucks (Harris *et al.* 2007; Lee *et al.* 2009). The aim of this paper is to address the bridge dynamics induced by crane type vehicles and how they compare to 5-axle articulated trucks for a variety of span lengths and road conditions. This information is of relevance to the road authorities giving permits to special heavy vehicles to drive along a specified route, and they must ensure that bridges will not suffer damage due to the passage of these abnormal traffic loads. This investigation focuses on the dynamic contribution of daily max crane-trucks using WIM records. Although most of the analysis is related to simply supported bridges, the dynamics of frame structure bridges with fixed supports are also discussed. The latter can be assumed to be an approximation for short spans of an integral form (culvert type). The possibility of a local damage adjacent to the expansion joint is considered here due to their frequent occurrence prior to the bridge (Kim *et al.* 2004; Lima, Brito 2009). Monte Carlo simulation is applied to the parameters of a 3D vehicle-bridge interaction (VBI) model to obtain bending moment effects for a wide range of vehicles with different mechanical characteristics, pavement conditions, expansion joints and bridge spans.

2. Selection of vehicle configuration

Vehicle data was recorded using a WIM system near Woerden in the Netherlands in 2005. There are 77 weekdays for which a full record is available, giving a total of 546 448 measured vehicles. Photographs from a roadside camera provided useful evidence to support the identification and classification of vehicle types. A significant feature of the gathered data is the high population of extremely heavy vehicles – cranes and low loaders – with a total of 892 vehicles in excess of 70 t, daily occurrences of vehicles over 100 t, and a recorded max of 165 t. Low loaders are characterized here by a group of closely-spaced axles at the front

ISSN 1822-427X print / ISSN 1822-4288 online
doi: 10.3846/bjrbe.2011.06
http://www.bjrbe.vgtu.lt

Fig. 1. Examples of recorded vehicles: a – 5-axle truck; b – large (mobile) crane

of the vehicle, followed by a gap of about 10 m and another group of axles at the rear. On the other hand, all axles on cranes are closely-spaced, and this concentration of weight over a much shorter wheelbase tends to produce higher bending moments on short to medium span bridges. Fig. 1 shows an example of a 5-axle truck and a typical crane. The 9-axle crane-truck in Fig. 1b has a gross vehicle weight (GVW) of 110.6 t and a wheelbase of 14.85 m. Cranes are frequently accompanied by vehicles carrying ballast which have gross weights and axle layouts that are very similar to the cranes.

The WIM data was employed to obtain the mid-span static bending moment for four bridge spans (7.5; 15; 25 and 35 m), and daily max for 5-axle articulated truck and crane loading events were stored. This led to eight different lists of 77 vehicles, for which the mean and standard deviations of the main recorded properties are shown in Table 1. These lists of 77 vehicles will be studied dynamically using a VBI model described in the section that follows.

3. Vehicle-bridge interaction model

3.1. Vehicle models

The 3D vehicle model used in this study consists of two major bodies, tractor and trailer, represented as lumped masses joined to the road or bridge surface by spring-dashpot systems, as shown in Fig. 2. Each axle is represented as a rigid bar with lumped masses at both ends that correspond to the wheel and suspension masses.

The general equation of motion to be solved for each vehicle is given by Eq(1):

$$M_v\ddot{z}_v(t) + C_v\dot{z}_v(t) + K_v z_v(t) = F_v(t), \quad (1)$$

where M_v, C_v and K_v – the vehicle mass, damping and stiffness matrices respectively; z_v – a vector containing the degrees of freedom of the vehicle; vector $F_v(t)$ contains the external forces applied to the system (Cantero *et al.* 2010). As cranes do not include a hinge, they are a special case of Fig. 2 with multiple tractor axles but no trailer. The vehicle model assumes constant speed, a tyre-ground point contact, vertical vehicle forces and linear stiffness and damping elements. Similar vehicle models have been widely used for modelling VBI (Green, Cebon 1995). Longitudinal wheel spacing, axle load distribution and speed of the vehicle models being tested are directly obtained from the recorded WIM data (Table 1), whereas 2 m transverse wheel distance is assumed. Tables 2 and 3 give other parameters adopted from the literature and the statistical variability assumed for their use in Monte Carlo simulations. For the 5-axle trucks, the type of drive suspension was assumed to be: air for 10% of the vehicles and steel for the remaining 90%; whereas an even distribution of air to steel suspension was assumed for trailer axles. Values of the suspension parameters are based on the analysis of 61 heavy vehicle suspensions by Fu and Cebon (2002). Tyre stiffness for drive and trailer wheels on 5-axle trucks is doubled, since articulated vehicles usually present double wheel configurations on these axles. The moments of inertia are calculated assuming a uniform mass distribution along the vehicle. The standard deviation of speed was increased with respect to recorded WIM values by 1.24 and 1.65 for 5-axle trucks and cranes respectively to cover for a wider range of speeds.

Table 1. Overview of vehicles characteristics large (mobile) cranes

	5-axle trucks		Large cranes	
	μ	σ	μ	σ
Number of axles	5.00	0.00	7.23	2.15
Gross vehicle weight, 10^3 kg	49.87	3.72	84.34	19.40
Axle load, 10^3 kg	9.97	0.74	7.53	2.28
Min axle spacing, m	1.34	0.05	1.47	0.16
Axle spacing, m	3.07	0.14	1.90	0.17
Max axle spacing, m	5.77	0.57	2.94	0.75
Wheelbase, m	12.30	0.58	11.89	4.35
Speed, km/h	85.47	3.70	79.69	5.67

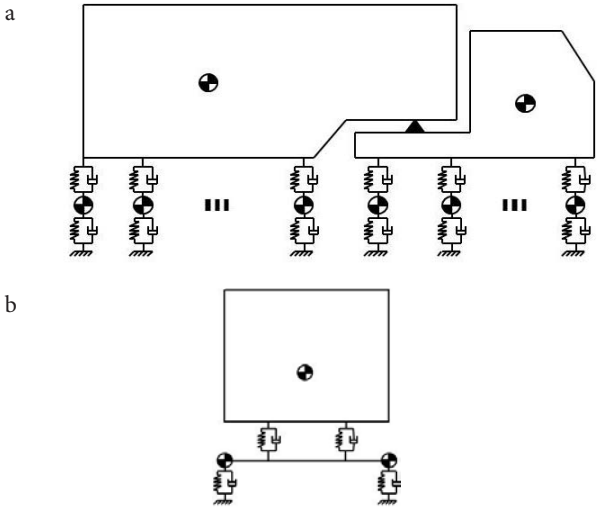

Fig. 2. General vehicle model: a – side elevation; b – cross-section

Table 2. 5-axle trucks parameters and variability

	Mean value, μ	Standard deviation, σ	Min	Max	Reference
Tractor sprung mass, kg	7000	1000	5000	9000	Harris *et al.* (2007)
Steer axle mass, kg	700	100	500	1 000	Harris *et al.* (2007); Fu and Cebon (2002); Kirkegaard *et al.* (1997)
Drive axle mass, kg	1000	150	700	1 300	
Trailer axles masses, kg	800	100	600	1 000	
Moments of inertia increase, %	0	25	–50	50	
Steer suspension stiffness, N/m	300×10^3	70×10^3	150×10^3	500×10^3	Fu and Cebon (2002)
Drive suspension stiffness (air), N/m	500×10^3	50×10^3	300×10^3	600×10^3	
Drive suspension stiffness (steel), N/m	1×10^6	300×10^3	600×10^3	1.5×10^6	
Trailer suspension stiffness (air), N/m	400×10^3	100×10^3	250×10^3	600×10^3	
Trailer suspension stiffness (steel), N/m	1.25×10^6	200×10^3	1×10^6	1.5×10^6	
Suspension viscous damping, Ns/m	5×10^3	2×10^3	3×10^3	10×10^3	Kirkegaard *et al.* (1997)
Tyre stiffness, N/m	735×10^3	200×10^3	500×10^3	1.5×10^6	Harris *et al.* (2007); Wong (1993)
Tyre damping, Ns/m	3×10^3	1×10^3	2×10^3	10×10^3	Kirkegaard *et al.* (1997)
Fifth wheel distance[a], m	0.65	0.10	0.50	1.30	Harris *et al.* (2007)
Suspension offset[b] (steer and trailer axles), m	0.10	0.05	0.08	0.30	Kirkegaard *et al.* (1997)
Suspension offset (drive axle), m	0.50	0.05	0.35	0.60	

Note: [a] – gap between the articulation and rear axle of tractor; [b] – distance between the wheel and the suspension support on the axle

Table 3. Crane type vehicles parameters and variability

	Mean value	Standard deviation	Min	Max	Reference
Axle mass, kg	700	300	500	1000	Harris *et al.* (2007)
Moments of inertia increase, %	0	25	–50	50	
Suspension stiffness, N/m	4×10^6	80×10^6	3×10^6	160×10^6	Li (2005)
Suspension damping, Ns/m	20×10^3	7.5×10^3	15×10^3	30×10^3	
Tyre stiffness, N/m	1×10^6	500×10^3	700×10^3	1.8×10^6	Lehtonen *et al.* (2006); Wong (1993)
Tyre damping, Ns/m	5×10^3	3×10^3	2×10^3	10×10^3	Lehtonen *et al.* (2006)

3.2. Bridge model

The bridge is modelled as an orthotropic thin plate following Kirchhoff's plate theory using the finite element technique for rectangular C_1 plate elements with four nodes (Rowley 2007). The element has four degrees of freedom at each node, namely one vertical displacement, two rotations and one torsion, adding up 16 degrees of freedom per element. Compared to the standard Kirchhoff plate element, this plate element contains one additional degree of freedom per node, included to prevent the discontinuity of the slope along the edge of the elements. Bridges with two boundary conditions are analysed: simply supported and fixed ends. The thickness and density of the plate elements are adjusted to represent the second moment of area and the distribution of mass of a typical bridge cross-section for each span under investigation. Five different concrete bridges have been modelled and their properties are listed in Table 4. Typical values of Young's modulus in the longitudinal direction of 3.5×10^{10} N/m^2, Poisson's ratio of 0.2, and a width of 11.3 m are assumed in all of them. The

properties for the shorter spans (7.5 and 15 m) are representative of solid slab decks made of inverted T beams and in-situ concrete according *Tarmac 2009: Prestressed Beams Technical Guide*. The properties of the longer spans (25 and 35 m) are based on beam-and-slab constructions, and they are modelled as orthotropic plates. The fundamental frequencies are found in agreement with those recorded in experimental observations (McLean, Marsh 1998). A 3% damping was applied to all modes of vibration.

The general equation of motion of a particular plate bridge model is given by Eq (2):

$$M_b\ddot{z}_b(t)+C_b\dot{z}_b(t)+K_bz_b(t)=F_b(t), \quad (2)$$

where M_b, C_b and K_b – the mass, damping and stiffness matrices respectively; $z_b(t)$ – a vector defining the motion of the plate nodes; $F_b(t)$ contains the external forces applied to the bridge finite element model (Rowley 2007).

3.3. Road profile

The road profile is generated as a stochastic process described by a power spectral density functions defined by *ISO 8608:1995 Mechanical Vibration – Road Surface Profiles – Reporting of Measured Data* together with the inverse fast Fourier transform method described by Cebon and Newland (1983). Road classes A (very good), B (good) and C (average) are investigated in this paper. The profiles are passed through a moving average filter to emulate the tyre contact patch (Harris *et al.* 2007). An expansion joint is integrated within this road profile. When the expansion joint is assumed to be in a healthy state, then, the road profile remains unaltered. But when the expansion joint is assumed to be damaged, it is modelled as a bump of a total width of 30 cm: a 10 cm length of gradual decrease down to 2 cm, a constant depression of 2 cm for another 10 cm and then, 10 cm of increase in height until reaching the road level (González *et al.* 2009). The 2 cm bump depth has been chosen following average values from expansion joints surveys on road networks from Japan (Kim *et al.* 2004) and Portugal (Lima, Brito 2009). These bumps are located at 0.5 m from bridge support to account for the usual beam overhang. Fig. 3 gives the profile resulting from combining a sample class B road profile and a 2 cm deep bump.

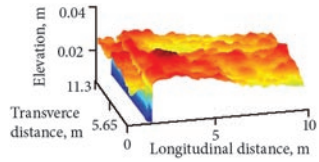

Fig. 3. Example of randomly generated class B road profile carpet combined with 2 cm bump

3.4. Dynamic interaction algorithm

An iterative procedure is employed to implement the interaction between the vehicle moving at constant speed and the bridge given an uneven road profile (Green, Cebon 1995). The steps involved in the iterative procedure are as follows:

- calculate vertical forces $F_v(t)$ for each vehicle due to motion over road profile using Eq (1);
- calculate vertical displacements of bridge ($z_b(t)$) due to vehicles forces ($F_v(t)$) using Eq (2);
- add bridge deformations ($z_b(t)$) to the original profile elevations ($r(t)$);
- recalculate vertical forces ($F_v(t)$) for the new profile ($z_b(t)+ r(t)$);
- repeat steps 2 to 4 until a tolerance value is reached.

In this paper, the stopping criterion is given by the relative difference in bending moment between two consecutive iterations becoming less than or equal to 0.1 %. Typically the solution takes 3 or 4 iterations. Note that this iteration process comprehends the complete solution in time for vehicle and bridge models for each iteration, whereas other alternative iterative procedures perform iterations stepwise (Green, Cebon 1995), searching for the tolerance value in every integration time step. The VBI algorithm described here was implemented using *MatLab* software. Each model, vehicle and bridge, can be solved independently and by means of different numerical integration schemes. The direct integration method Newmark-β is used to calculate vehicle responses over profiles. The plate displacements due to the external loads are calculated by means of the exponential matrix method and approximating the forcing function as a piecewise linear function that leads to an explicit integration formula. The results of

Table 4. Bridge models properties

Span, m	Boundary condition	Thickness, m	Density, kg/m^3	Transversal Young's modulus, N/m^2	1st longitudinal natural frequency, Hz	1st torsional natural frequency, Hz
7.5	Simply supp.	0.45	2 400	3.50×10^{10}	14.02	19.06
7.5	Fixed	0.45	2 400	3.50×10^{10}	31.91	34.97
15	Simply supp.	0.85	2 400	3.50×10^{10}	6.59	13.92
25	Simply supp.	1.40	1 800	1.40×10^{10}	4.40	12.02
35	Simply supp.	1.80	1 400	1.25×10^{10}	3.24	11.66

the algorithm employed here were found to compare favourably with other alternative VBI procedures (González *et al.* 2008), and it was selected because of its computational efficiency.

4. Monte Carlo simulation

In this section, single vehicle events and meeting vehicle events are studied separately for bidirectional traffic bridges. Each lane is 3.65 m wide with additional 2 m kerbs. Vehicles travel over a min road approach of 100 m before entering the bridge. Fig. 4 shows the paths of the wheels on the structure together with the location of the expansion joints.

Static and total bending moments are studied at 3 points along mid-span marked in Fig. 4. Dynamic amplification factor (DAF) is used to quantify the increase in load effect due to VBI and it is defined as the ratio of max total bending moment to max static bending moment taken into account the 3 points under investigation (i.e., the point holding the max moment may vary depending on the traffic loading event).

4.1. Single vehicle events

The loading effects of the 77 different daily max vehicles (Section 2), for 2 vehicle types (5-axle trucks and cranes) are analysed for 4 simply supported spans (Table 4) with 2 expansion joint conditions (healthy and damaged). Monte Carlo simulation is used to cover for the large variability in dynamic properties of a vehicle. Over 300 000 single vehicle events are simulated to characterise the mid-span bending moment statistically. The vehicle parameters are randomly sampled from normal distributions while maintaining the values within reasonable thresholds (Tables 1–3). The road profiles are also randomly generated based on PSD functions recommended by *ISO 8608:1995. Mechanical Vibration – Road Surface Profiles – Reporting of Measured Data* for road classes A, B and C. The typical values of air and steel suspensions used for 5-axle trucks in the Monte Carlo simulation leads to the DAF values for a road class B shown in Fig. 5. Air suspensions originate smaller and less disperse dynamic effects on the bridge than steel leaf spring suspensions as expected given the "road-friendly" nature of softer suspensions according *SAMARIS 2006: Guidance for the Optimal Assessment of Highway Structures*.

Fig. 6 compares the mean DAF value for each of the 77 articulated trucks and 77 cranes being tested when driven over a class B surfaces. It can be seen that 5-axle trucks generally generate higher dynamics as result of their lighter GVW and larger axle spacings. These results are found in agreement with prior experimental findings in *SAMARIS 2006 and ARCHES 2009: Assessment and Rehabilitation of Central European Highway Structures*.

Fig. 7 shows the standard deviation associated to the mean values in Fig. 6. This standard deviation appears to be smaller for crane type vehicles. Therefore, DAF is not only typically lower for crane-trucks than 5-axle trucks, but also less scattered.

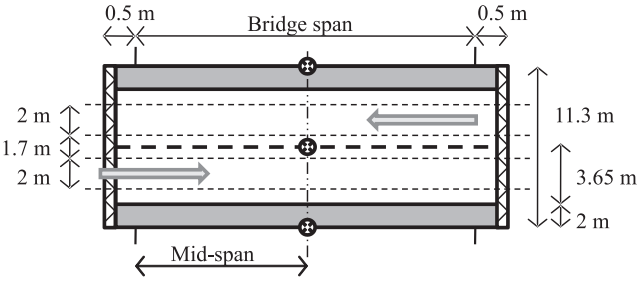

Fig. 4. Plan view of bridge showing wheel paths (– – –), expansion joints (▭) and moment locations under study (⊕)

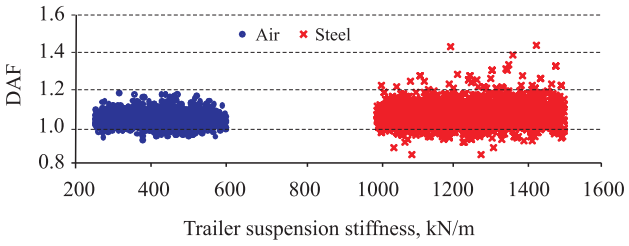

Fig. 5. DAF for 5-axle trucks on simply supported 25 m bridge for class B road profiles and no bump prior to the bridge for trailer air (•) and steel (×) suspension

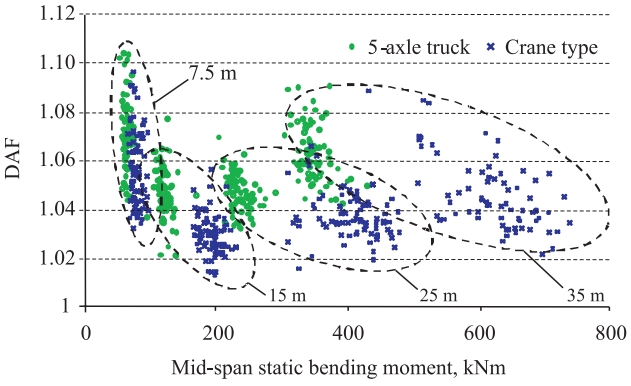

Fig. 6. Mean DAF for vehicles over class B profiles and healthy expansion joint. Results for each span are surrounded within corresponding curve (dashed line)

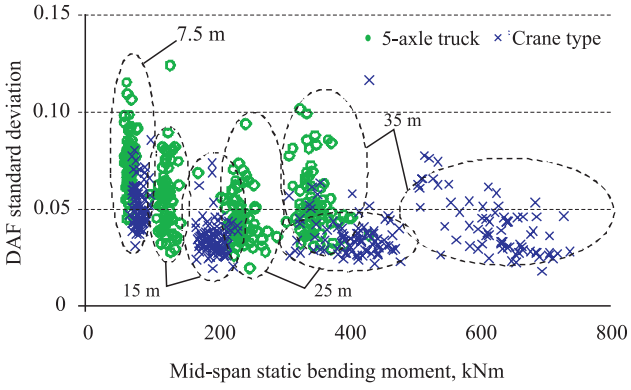

Fig. 7. DAF standard deviation for vehicles over class B profiles and healthy expansion joint. Results for each span are included in corresponding curve (dashed line)

The dynamic increment (DI) due to the presence of a damaged expansion joint is defined here as the difference in DAF between the presence of a 2 cm bump due to defect in joint (Section 3) and the absence of a bump. Fig. 8 presents DI due to the bump for 5-axle trucks and cranes over class B road surfaces and four spans. Results show that the bump only has relevant influence on the mid-span bending moment of the shortest span (7.5 m), in particular for 5-axle trucks. The difference in DI values between articulated trucks and cranes for the 7.5 m span is due to the longer wheelbases and pitch moments of inertia of cranes, thus being affected very little by local discontinuities on the pavement.

Similar trends in mean (μ) and standard deviation (σ) of DAF values are obtained for other road classes and expansion joints, and they are summarized in Table 5. As expected and indicated in *DIVINE 1998: Dynamic Interaction between Vehicles and Infrastructure Experiment*, DAF increases with road roughness more significantly for shorter spans and 5-axle trucks. Only for 7.5 m spans the effect of a 2 cm bump on DAF is relevant, and it is equivalent to have a poorer road class condition than the PSD may indicate. For longer spans than the 7.5 m bridge, the influence of the 2 cm bump is not so important. It must be noted that in some special combinations of vehicle properties and road profile, the bump may have a favourable load effect that reduces the mid-span moment.

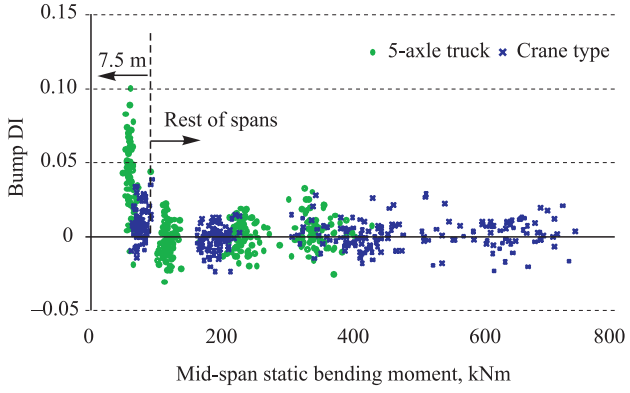

Fig. 8. Bump dynamic increment for vehicles on class B roads

Cranes may govern the assessment of traffic load effects in short to medium simply supported bridges due to its large GVW distributed within very closely spaced axles. The results in this section have shown that the DAF associated to cranes is considerably smaller and also less scattered than the DAF associated to the more common 5-axle truck.

Cranes may govern the assessment of traffic load effects in short to medium simply supported bridges due to its large GVW distributed within very closely spaced axles. The results in this section have shown that the DAF associated to cranes is considerably smaller and also less variable than the DAF associated to the more common 5-axle truck.

4.2. Meeting events

Two or more heavy trucks can also meet on a two-lane bridge leading to a critical traffic loading scenario (González *et al.* 2008). Three types of meeting events are modelled here to compare different traffic scenarios. Type I is defined as a typical situation of two heavy 5-axle trucks meeting on a bridge, type II refers to a 5-axle truck meeting a crane (that could be avoided if appropriate escort is provided), and type III refers to an unlikely and hypothetical two-crane event. Over 180 000 meeting events were generated using Monte Carlo simulation for a variety of spans, profile classes, expansion joints, meeting types, ve-

Table 5. Mean (μ) and standard deviation (σ) for DAF results from Monte Carlo simulation of single vehicle events

Span, m	Vehicle type	Standard value	No bump			2 cm bump		
			Profile class					
			A	B	C	A	B	C
7.5	5-axle	μ	1.048	1.072	1.146	1.096	1.112	1.171
		σ	0.043	0.075	0.151	0.070	0.096	0.162
	Crane	μ	1.052	1.058	1.091	1.059	1.067	1.097
		σ	0.036	0.052	0.098	0.037	0.054	0.096
15	5-axle	μ	1.036	1.048	1.086	1.035	1.045	1.082
		σ	0.032	0.056	0.103	0.033	0.055	0.097
	Crane	μ	1.021	1.030	1.057	1.020	1.028	1.057
		σ	0.021	0.035	0.066	0.021	0.036	0.067
25	5-axle	μ	1.034	1.047	1.095	1.033	1.048	1.094
		σ	0.031	0.045	0.084	0.030	0.046	0.087
	Crane	μ	1.024	1.038	1.078	1.023	1.037	1.078
		σ	0.021	0.035	0.067	0.022	0.037	0.067
35	5-axle	μ	1.040	1.064	1.129	1.041	1.067	1.133
		σ	0.033	0.053	0.102	0.033	0.055	0.103
	Crane	μ	1.025	1.046	1.099	1.027	1.049	1.105
		σ	0.023	0.042	0.084	0.025	0.043	0.084

hicles, vehicle characteristics and meeting locations on the bridge. Fig. 9 shows the average DAFs for two vehicles meeting on a 25 m bridge. There is a clear trend of decreasing dynamic excitation with increasing static load effect.

Table 6 presents mean and standard deviations of DAF values for all meeting events. The dynamic excitation increases with road roughness for every span and meeting event type, although DAF values are smaller for those meeting event involving heavier vehicles. These conclusions are consistent with previous experimental by *SAMARIS 2006 and ARCHES 2009*, and simulated results (González *et al.* 2008). The influence of the bump in meeting events is in general much smaller than for single vehicle events (Table 5); and as for single events, it is only important for the 7.5 m span.

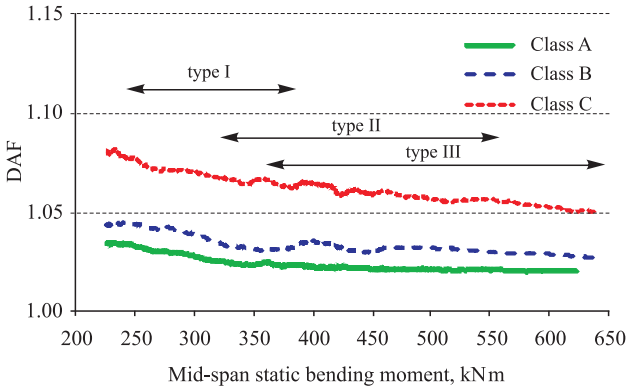

Fig. 9. Average DAF values for meeting events over 25m span bridge without bump. Arrows indicate the range where specified meeting event types apply

4.3. Influence of the bridge boundary conditions

All bridges in previous sections were simply supported (SS), however, a significant proportion of short span bridges are frame constructions with a deck behaviour close to fixed end structures. For this reason, simulations are carried out here restraining rotations at both ends of the 7.5 m span bridge, and the results are compared to those obtained for the simply supported case for a road class B (Section 4.1). In the case of fixed-fixed (FF) bridges there is significant bending moment at mid-span, as well as at the supports, and both DAFs are evaluated. Fig. 10 presents the mean DAF values for each single vehicle event separated in terms of bridge boundary condition (SS and FF), section under consideration (mid-span and support) and vehicle type (5-axle or crane truck). It can be seen how fixed structures prevent large dynamic oscillations, and DAF values found in fixed structures are considerably smaller than in the simply supported case. Furthermore, in the fixed structure, the DAF values and load effects at mid-span are generally smaller than at the supports.

Table 6. Mean (μ) and standard deviation (σ) for DAF results from Monte Carlo simulation of meeting events

Span, m	Meeting type	Standard value	No bump			2 cm bump		
			Profile class					
			A	B	C	A	B	C
7.5	type I	μ	1.024	1.034	1.071	1.069	1.074	1.093
		σ	0.031	0.045	0.099	0.051	0.057	0.098
	type II	μ	1.025	1.032	1.056	1.050	1.054	1.070
		σ	0.029	0.042	0.074	0.040	0.051	0.081
	type III	μ	1.030	1.032	1.054	1.036	1.041	1.057
		σ	0.031	0.040	0.070	0.029	0.039	0.068
15	type I	μ	1.024	1.029	1.049	1.023	1.025	1.041
		σ	0.028	0.041	0.069	0.027	0.045	0.074
	type II	μ	1.022	1.026	1.048	1.021	1.026	1.044
		σ	0.020	0.033	0.057	0.020	0.030	0.056
	type III	μ	1.020	1.025	1.040	1.018	1.023	1.041
		σ	0.019	0.030	0.053	0.017	0.028	0.053
25	type I	μ	1.023	1.030	1.061	1.027	1.032	1.053
		σ	0.023	0.033	0.059	0.022	0.035	0.056
	type II	μ	1.022	1.030	1.055	1.024	1.030	1.053
		σ	0.016	0.026	0.050	0.017	0.026	0.048
	type III	μ	1.020	1.028	1.051	1.020	1.027	1.049
		σ	0.016	0.026	0.045	0.016	0.025	0.047
35	type I	μ	1.028	1.042	1.077	1.030	1.043	1.080
		σ	0.024	0.040	0.070	0.024	0.038	0.072
	type II	μ	1.022	1.036	1.066	1.024	1.035	1.072
		σ	0.016	0.029	0.056	0.019	0.030	0.057
	type III	μ	1.021	1.033	1.065	1.023	1.033	1.062
		σ	0.016	0.026	0.048	0.018	0.028	0.049

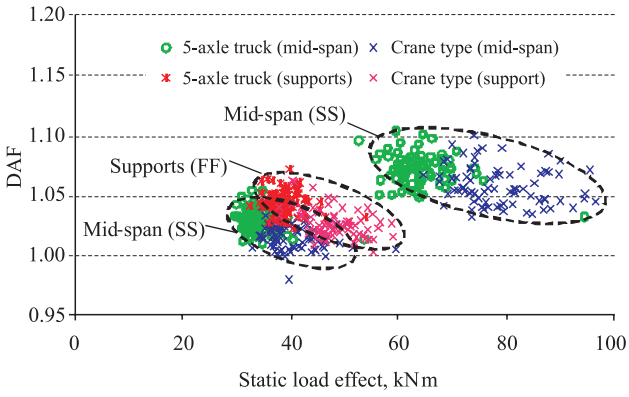

Fig. 10. Comparison of mean DAFs for 7.5 m span bridge and class B profile without bump

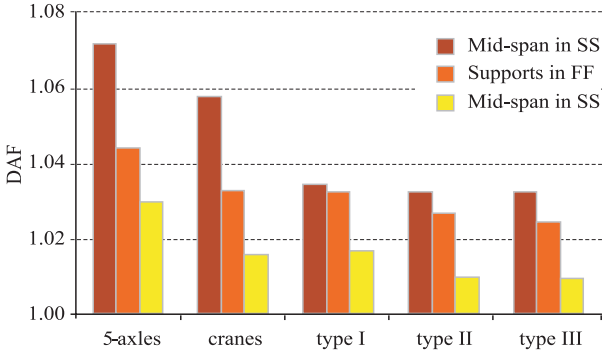

Fig. 11. Average DAF values for 7.5 m span bridge, subdivided into different vehicle fleets and meeting events (class B and no bump)

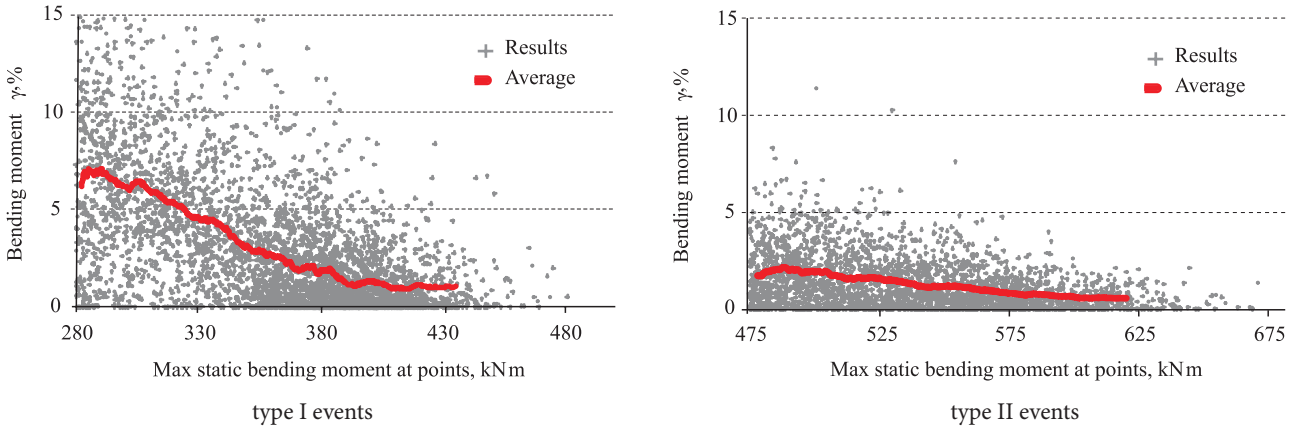

Fig. 12. Gamma values on 25 m span

Fig. 11 compares the mean DAF values obtained for single and meeting vehicle events on a 7.5 m bridge with class B road roughness and two boundary conditions. DAF values decrease as load effect increases, being the fixed bridge less sensitive to dynamic amplification than the simply supported structure.

4.4. Max total moment on the bridge

The max total bending moment due to a moving sprung model on a simply supported beam does not necessarily occur at mid-span (Cantero *et al.* 2009). A simple way to evaluate the difference between the actual largest bending moment (anywhere in the bridge) and the mid-span bending moment, is as a percentage of the latter, denoted here as γ. Fig. 12 presents γ values using the results of Monte Carlo simulation for types I and II meeting events. Even though large percentages are observed, the values decrease considerably with increasing static load. Similar trends are observed for other span lengths and traffic events.

5. Conclusions

This paper has investigated the dynamic amplification of the bridge response due to the passage of 5-axle trucks and cranes for short to medium span lengths. Past investigations on the total response of 5-axle trucks have found that the heavier the truck mass, the larger the total load effect but generally the smaller the increase in dynamic amplification. The passage of a crane is a far more critical loading situation than a 5-axle truck for a single span due to its heavier and more concentrated load, but the dynamic amplification of a bridge caused by a crane has not received sufficient attention in the literature. The results in this paper have shown that the large mass and rigid configuration of the crane leads to a small dynamic excitation of the bridge compared to the articulated 5-axle truck. The crane is also less sensitive to damaged expansion joints than the 5-axle articulated truck. Four bridge span lengths have been tested (7.5; 15; 25 and 35 m) and the influence of a local discontinuity due to a defect of the expansion joint has only been significant for the shortest span. Similar conclusions have been reached when considering two trucks meeting on the bridge; however DAF values for meeting events are generally smaller than for single vehicle events. Therefore, an accurate assessment of bridge safety regarding the crossing of a bridge by a large crane, should take into account an appropriate dynamic factor for a crane-type vehicle in single vehicle situations or meeting events.

For well maintained road surfaces (classes A and B), simulations suggest a DAF reference value of 1.05 when

assessing large cranes crossing simply supported spans between 7.5 and 35 m. This value of DAF can be defined more accurately based on the exact vehicle/s involved in the critical loading scenario under investigation, the bridge and the profile. If there was a damaged expansion joint, some additional dynamic allowance should be added for spans shorter than 15 m. *Eurocode EN 1991-2 Actions on Structures – Part 2: Traffic Loads on Bridges* necessarily uses conservative DAF values of 1.27, 1.24, 1.2 and 1.16 built in the traffic model for two-lane 7.5, 15, 25 and 35 m bridge spans respectively to cover for a wide range of scenarios. These DAF values are higher for one-lane bridges, where the Eurocode applies 1.625 to the traffic load model for a 7.5 m span length, and 1.4 to the models for 15, 25 and 35 m span lengths. This paper has shown that these values proposed by the Eurocode can be considerably smaller in a situation of low dynamic excitation, such as a large crane travelling on a very good road profile over a short span bridge.

When the response at mid-span section is taken as reference in simulations or measurements, it must be taken into account that it may not be the section holding the highest bending moment. Therefore, the DAF results at mid-span should be increased by a small percentage that tends to decrease rapidly with increasing static load effect.

It has been shown that the boundary conditions of a bridge play a fundamental role in its dynamic allowance. The bending moments of a 7.5 m frame structure bridge with fixed supports has resulted in considerably smaller DAF values than those associated to a 7.5 m simply supported bridge. Therefore, if the structure is fully restrained at the supports, the section at the support has shown to be a more critical location than the mid-span section, both statically and dynamically.

Acknowledgements

The authors would like to express their gratitude for the financial support received from the 6th European Framework Project ARCHES (Assessment and Rehabilitation of Central European Highway Structures) towards this investigation. The authors would also like to gratefully acknowledge the assistance of the Rijkswaterstaat Centre for Transport and Navigation (DVS), an advisory institute of the Dutch Ministry of Transport, Public Works and Water Management in the Netherlands, who provided the WIM data.

References

Cantero, D.; OBrien, E. J.; González, A. 2010. Modelling the Vehicle in Vehicle–Infrastructure Dynamic Interaction Studies, in *Proceedings of the Institution of Mechanical Engineers, Part K: Journal of Multi-Body Dynamics* 224(2): 243–248. doi:10.1243/14644193JMBD228

Cantero, D.; González, A.; OBrien, E. J. 2009. Maximum Dynamic Stress on Bridges Traversed by Moving Loads, in *Proceedings of the ICE - Bridge Engineering* 162 (BE2): 75–85 doi:10.1680/bren.2009.162.2.75

Cebon, D.; Newland, D. E. 1983. Artificial Generation of Road Surface Topography by the Inverse F.F.T. Method, *Vehicle System Dynamics* 12(1–3): 160–165. doi:10.1080/00423118308968747

Fu, T. T.; Cebon, D. 2002. Analysis of Truck Suspension Database, *International Journal of Heavy Vehicle Systems* 9(4): 281–297. doi:10.1504/IJHVS.2002.001180

González, A.; Rattigan, P.; OBrien, E. J.; Caprani, C. 2008. Determination of Bridge Lifetime Dynamic Amplification Factor Using Finite Element Analysis of Critical Loading Scenarios, *Engineering Structures* 30(9): 2330–2337. doi:10.1016/j.engstruct.2008.01.017

Green, M. F.; Cebon, D. 1995. Dynamic Interaction between Heavy Vehicles and Highway Bridges, *Computers & Structures* 62(2): 253–264. doi:10.1016/S0045-7949(96)00198-8

Green, M. F.; Cebon, D.; Cole, D. J. 1995. Effects of Vehicle Suspension Design on Dynamics of Highway Bridges, *Journal of Structural Design* 121(2): 282–272. doi:10.1061/(ASCE)0733-9445(1995)121:2(272)

Harris, N. K.; OBrien, E. J.; González, A. 2007. Reduction of Bridge Dynamic Amplification through Adjustment of Vehicle Suspension Damping, *Journal of Sound and Vibration* 302(3): 471–485. doi:10.1016/j.jsv.2006.11.020

Kirkegaard, P. H.; Nielsen, S. R. K.; Enevoldsen, I. 1997. *Heavy Vehicles on Minor Highway Bridges – Dynamic Modelling of Vehicles and Bridges*. Research Report R9721. Aalborg University, Department of Building Technology and Structural Engineering. 37 p.

Kim, C. W.; Kawatani, M.; Hwang, W.-S. 2004. Reduction of Traffic-Induced Vibration of Two-Girder Steel Bridge Seated on Elastomeric Bearings, *Engineering Structures* 26(14): 2185–2195. doi:10.1016/j.engstruct.2004.08.002

Lee, Y. S.; Kim, S. H.; Skibniewski, M. J. 2009. Analytical and Experimental Approach for Assessing Vibration Serviceability of Highway Bridges due to Heavy Vehicle Traffic, *The Baltic Journal of Road and Bridge Engineering* 4(3): 123–133. doi:10.3846/1822-427X.2009.4.123-133

Lehtonen, T.; Kaijalainen, O.; Pirjola, H.; Juhala, M. 2006. Measuring Stiffness and Damping Properties of Heavy Tyres, in *Proc. of the FISITA World Automotive Congress*. October 22–27, 2006, Yokohama, Japan.

Li, H. 2005. *Dynamic Response of Highway Bridges Subjected to Heavy Vehicles*. PhD thesis. Florida State University. 146 p.

Lima, J. M.; Brito, J. 2009. Inspection Survey of 150 Expansion Joints in Road Bridges, *Engineering Structures* 31(5): 1077–1084. doi:10.1016/j.engstruct.2009.01.011

McLean, D. I.; Marsh, M. L. 1998. *Dynamic Impact Factors for Bridges*, NCHRP Report 266, Transportation Research Board: Washington D.C. p. 66. ISSN 0547-5570.

OBrien, E. J.; Žnidarič, A.; Ojio, T. 2008a. Bridge-Weigh-in-Motion – Latest Developments and Applications Worldwide, in *Proc. of the International Conference of Heavy Vehicles.* May 19–22, 2008, Paris, France. 39–56.

OBrien, E.; Enright, B.; Caprani, C. 2008b. Implications of Future Heavier Trucks for Europe's Bridges, in *Transport Research Arena Europe*. April 21–25, 2008, Ljubljana, Slovenia.

O'Connor, A.; Eichinger, E. V. 2007. Site-specific Traffic Load Modelling for Bridge Assessment, *ICE Journal of Bridge Engineering* 160(4): 185–194. doi: 10.1680/bren.2007.160.4.185

Rowley, C. W. 2007. *Moving Force Identification of Axle Forces on Bridges*. PhD thesis. University College Dublin, Ireland. 325 p.

Wong, J. Y. 1993. *Theory of Ground Vehicles*. 2nd edition. New York: John Wiley & Sons. 528 p. ISBN 0471354619.

Received 12 January 2010; accepted 17 February 2011